Exploring the limits of EEG

-time, space & content

EEG signals reflect information processing by a complex organ trying to manage a complex environment

EEG based inference will always be extremely ill-posed

Strong priors are needed!

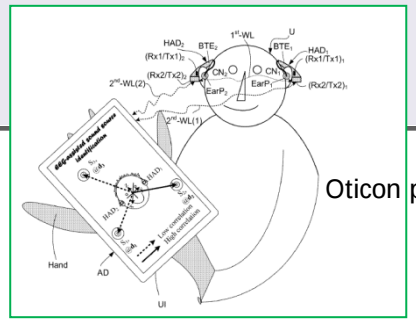

Oticon patent

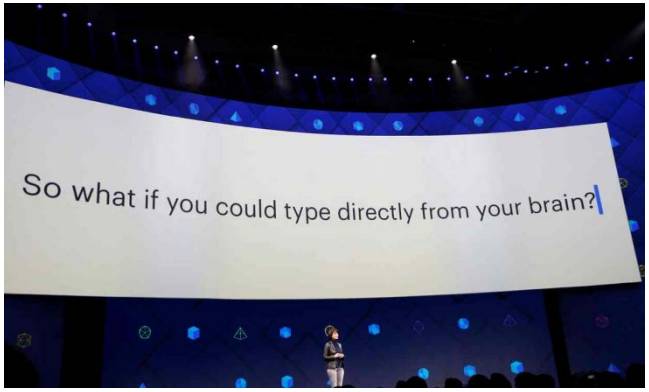

Lars Kai Hansen
DTU Compute,
Technical University of Denmark
lkai@dtu.dk

“Facebook has 60 people working on how to read your mind

According to FB it’s developing technology to read your brainwaves so that you don’t have to look down at your phone to type emails, you can just think them.”

Guardian April 19, 2017

Long term aim of neurotechnology…

Connect cognitive neuroscience and normal behavior

Conventional EEG system

High-performance research and clinical EEG system

Wearable EEG system

Discreet, unobtrusive and user-friendly assistive devices for everyday life

Ear-EEG/Hyposafe device

Smartphone data

Brain state representations connected by machine learning

”We don’t really know which, when or why brain states occur in the wild….”

Oticon mobile EEG device

(19) **United States**
(12) **Patent Application Publication**
LUNNER

(10) **Pub. No.: US 2016/0081623 A1**
(43) **Pub. Date: Mar. 24, 2016**

(54) **HEARING ASSISTANCE SYSTEM COMPRISING ELECTRODES FOR PICKING UP BRAIN WAVE SIGNALS**

(71) Applicant: **Oticon A/S**, Smorum (DK)

(72) Inventor: **Thomas LUNNER**, Smorum (DK)

(73) Assignee: **Oticon A/S**, Smorum (DK)

(52) **U.S. Cl.**
CPC ***A61B 5/6817*** (2013.01); ***G06F 3/015*** (2013.01); ***H04R 25/65*** (2013.01); ***H04R 25/554*** (2013.01); ***A61B 5/0478*** (2013.01); ***A61B 5/0006*** (2013.01); ***A61B 5/0024*** (2013.01); *H04R 2225/61* (2013.01); *A61B 2560/0468* (2013.01)

(57) **ABSTRACT**

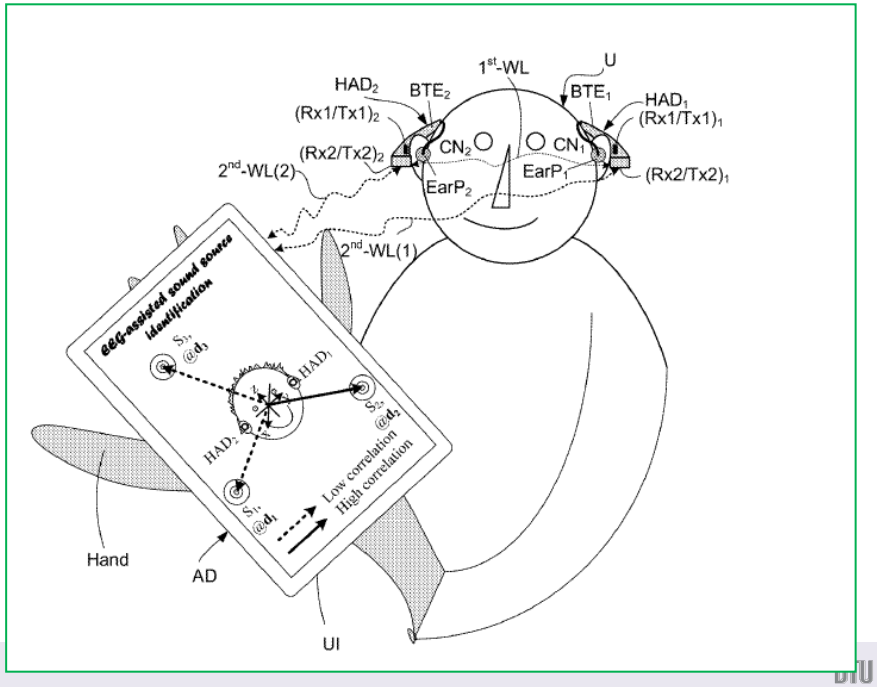

Lars Kai Hansen
DTU Compute, Technical University of Denmark

Exploring the limits to EEG

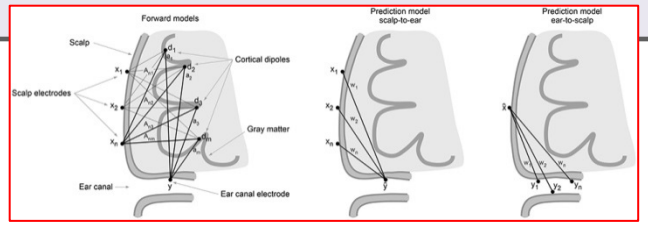

System level

Time & space – where and how long...

towards permanent EEG: - UNEEG, ear-EEG

smartphone brain scanner II

Content – what are the limits to mindreading?

EEG in the classroom

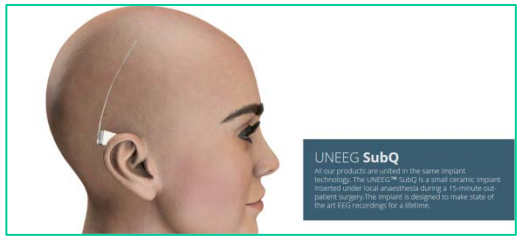

Brain level

Time & space – spatio-temporal resolution of EEG?

Bayesian inference with priors – infer forward model

Content – deep decoding with personal priors

Smartphone brain scanner III

Systems level limits:

Time & space EEG - where and how long...?

Expanding the reach of EEG: Ear-EEG and UNEEG

Extended recording in the wild:"Neurotechnology for 24/7 brain monitoring"
- naturalistic condition brain imaging experiments

Medical applications: Hypoglemia, epilepsia, sleep, …

Well-being: Hearing, attention, sleep scoring
resting state/mind wandering

P. Kidmose et al. Auditory Evoked Responses from Ear-EEG Recordings. IEEE EMBS (2012)

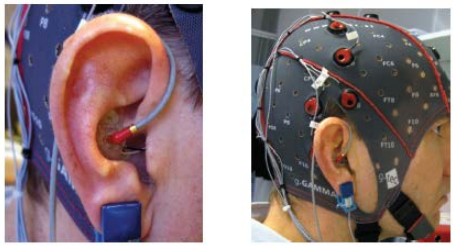

(c) Right ear with earplug. (d) Side view of test subject showing the recording setup.

Fig. 1. View of a right ear earplug and the Ear-EEG recording setup.

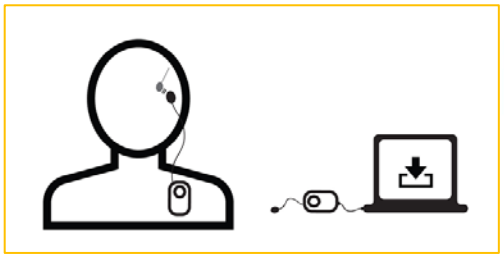

UNEEG **SubQ**

All our products are united in the same implant technology. The UNEEG™ SubQ is a small ceramic implant inserted under local anaesthesia during a 15-minute out-patient surgery. The implant is designed to make state of time.

UNEEG™ medical – formerly HypoSafe - was founded in 2005 by Henning Beck-Nielsen a leading diabetes scientists, with a mission to help individuals suffering from hypoglycemic attacks. Beck-Nielsen found that hypoglycemia could be predicted timely and reliably from the EEG patterns in the brain. **https://www.uneeg.com/**

UNEEG device ultra-long EEG - mental state predictability

Fano Ineq. bound on predictability of spectral microstates (ts=1 sec)

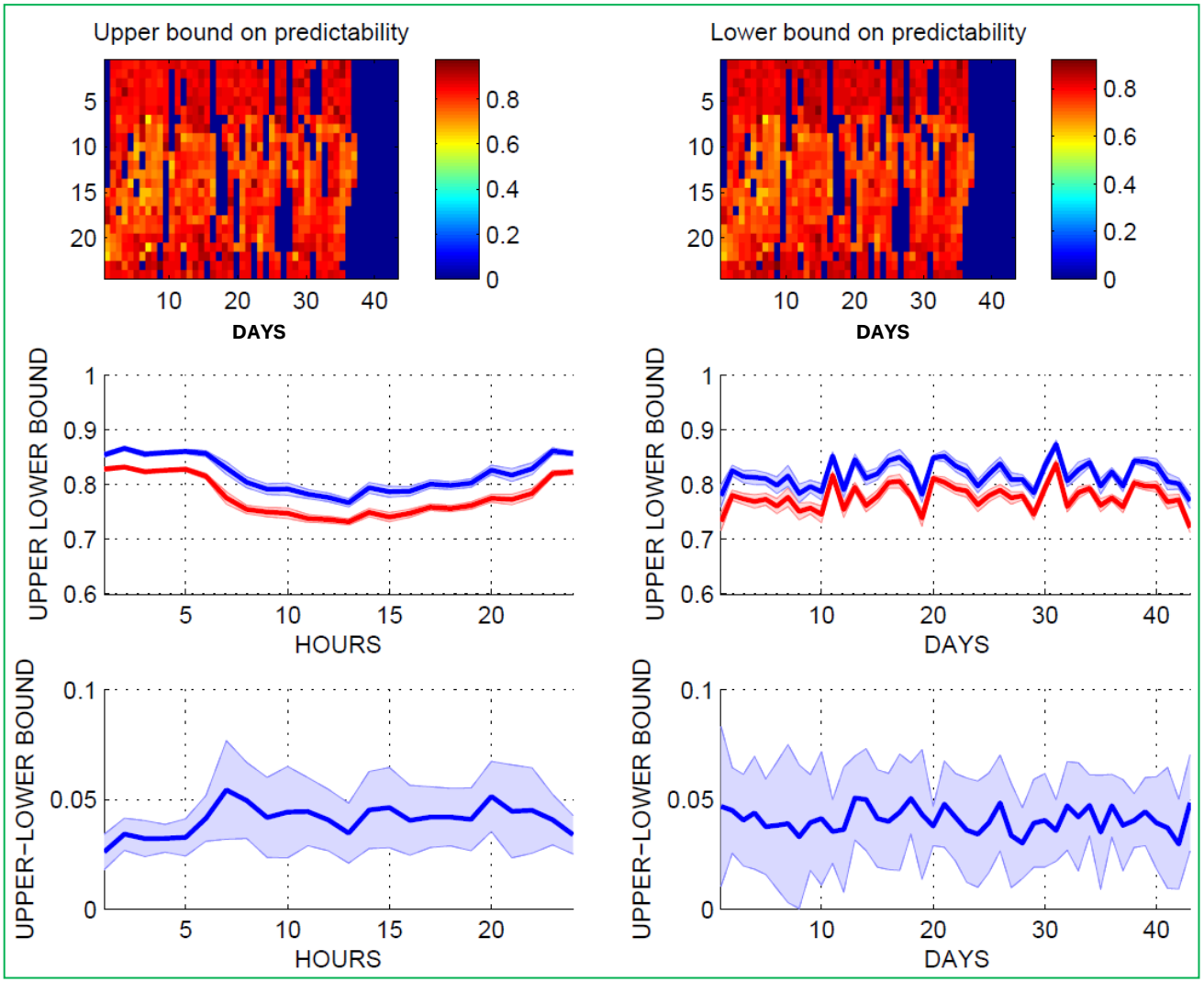

Predictability is
high at night,
lowest during ”leisure time”

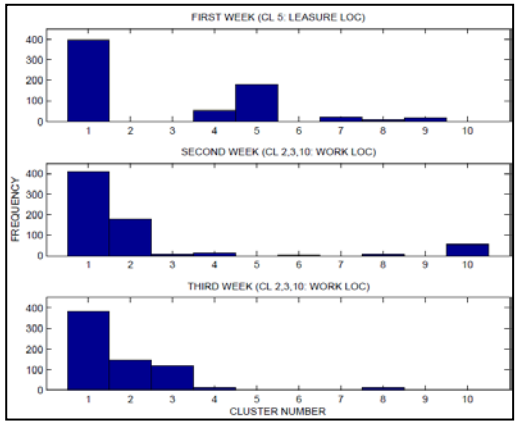

Lars Kai Hansen
DTU Compute, Technical University of Denmark

Establish strong priors for Ear-EEG decoding by linking EEG from scalp and ear

frontiers in Human Neuroscience
METHODS
published: 30 June 2017
doi: 10.3389/fnhum.2017.00341

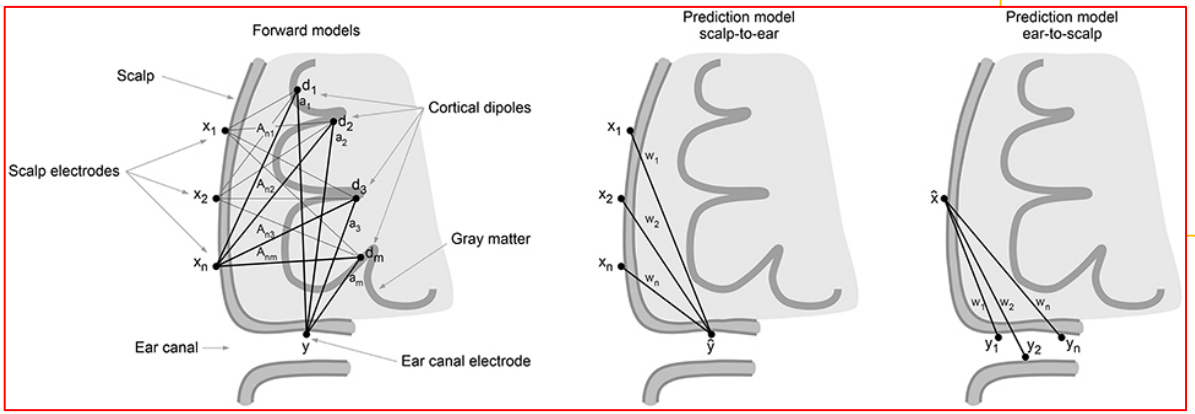

On the Keyhole Hypothesis: High Mutual Information between Ear and Scalp EEG

*Kaare B. Mikkelsen[1], Preben Kidmose[1] and Lars K. Hansen[2]**

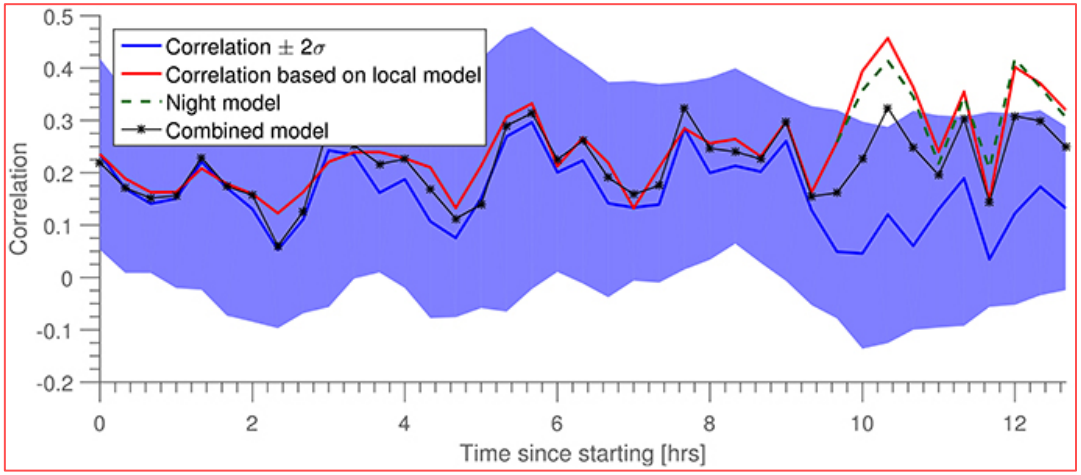

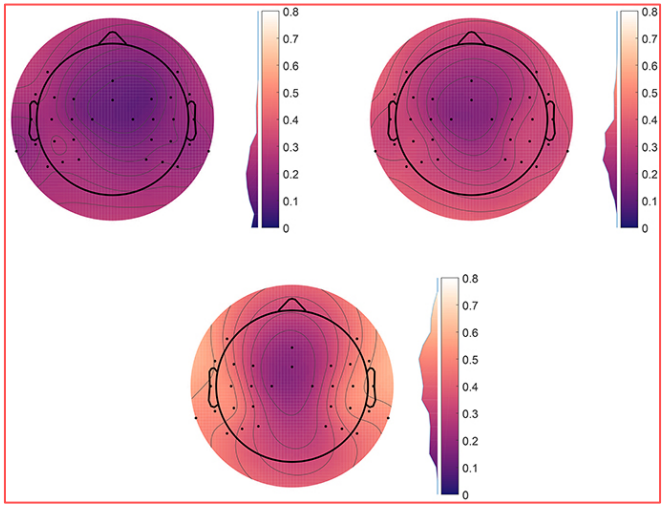

Mikkelsen, K.B., Kidmose, P. and Hansen, L.K., 2017. On the Keyhole Hypothesis: High Mutual Information between Ear and Scalp EEG. *Frontiers in human neuroscience*, *11*, p.341.

Systems level limits:

3D imaging & content decoding beyond the lab

Smartphone brain scanner II

Lars Kai Hansen
DTU Compute, Technical University of Denmark

Why 3D real-time imaging?

Enable on-line visual quality control

Neurofeed applications can be based on activity in specific brain structures /networks

Context priors may relate to 3D location (from meta analysis)

Evidence that BCI /decoding can be improved by 3D representation

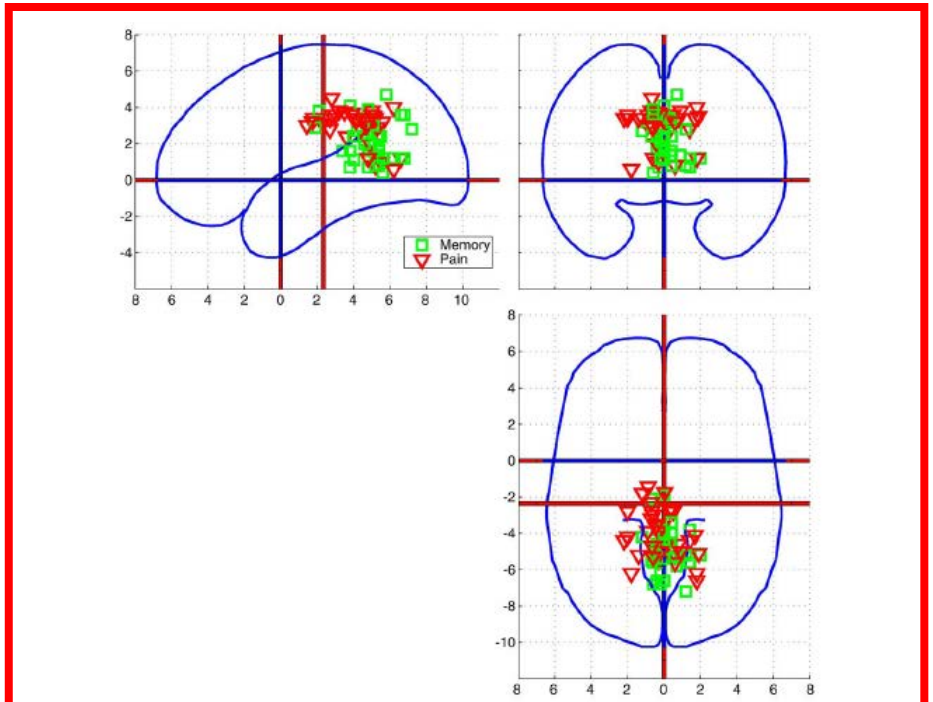

Fig. 3. Distribution of memory and pain brain activations in the posterior cingulate cortex shown on a sagittal plot: y is the AP axis with posterior as negative. The blue outline follows that of the Talairach atlas. The gray outline is an isocurvature in a probability volume for posterior cingulate cortex based on modeling of coordinates from the Brede database. Green squares are associated with "memory" articles and red triangles with "pain" articles.

Finn Årup Nielsen, Daniela Balslev, Lars Kai Hansen, "Mining the Posterior Cingulate: Segregation between memory and pain components". NeuroImage, 27(3):520-532, (2005)

Trujillo-Barreto, Nelson J., Eduardo Aubert-Vázquez, and Pedro A. Valdés-Sosa. "Bayesian model averaging in EEG/MEG imaging." NeuroImage 21, no. 4 (2004): 1300-1319.

Source representation can improve decoding

Besserve et al. (2011)

... reconstructing the underlying cortical network dynamics significantly outperforms a usual electrode level approach in terms of information transfer and also reduces redundancy between coherence and power features, supporting a decrease of volume conduction effects. Additionally, the classifier coefficients reflect the most informative features of network activity, showing an important contribution of localized motor and sensory brain areas, and of coherence between areas up to 6 cm distance.

Ahn et al. (2012)

... source imaging may enable noise filtering, and in so doing, make some invisible discriminative information in the sensor space visible in the source space.

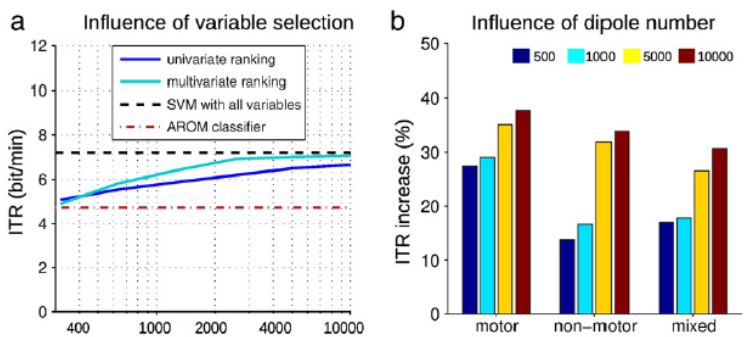

Fig. 6. Effect of reducing the number of sources or variables, for *power+coherence* quantification at the source level. a) Average ITR as a function of the number of variables for two variable ranking techniques: univariate ranking with a Student's *t*-test and multivariate ranking with the coefficient of a SVM classifier. The ITR values using a sparse number of variables with the AROM classifier (see text) and all variables with an SVM are plotted for comparison. b) Influence of the number of cortical dipoles used in the forward model on the ITR: percentage improvement of ITR with respect to electrode level quantification, for each type of couples of tasks (motor, non-motor and mixed couples).

Congedo, Marco, Fabien Lotte, and Anatole Lécuyer. "Classification of movement intention by spatially filtered electromagnetic inverse solutions." *Physics in Medicine and Biology* 51, no. 8 (2006): 1971

M Besserve, J Martinerie, L Garnero "Improving quantification of functional networks with eeg inverse problem: Evidence from a decoding point of view." *NeuroImage* 55.4 (2011): 1536-1547.

Minkyu Ahn, Jun Hee Hong, Sung Chan Jun: "Feasibility of approaches combining sensor and source features in brain–computer interface." *Journal of Neuroscience Methods* 204 (2012): 168-178.

Andersen, R.S., Eliasen, A.U., Pedersen, N., Andersen, M.R., Hansen, S.T. and Hansen, L.K., EEG source imaging assists decoding in a face recognition

Smartphone brain scanner at YouTube

https://www.youtube.com/watch?v=i_66KAOzXhU

Limits to imaging

Linear, ill-posed inverse problem

X: N x T
Y: K x T
A: K x N

N >> K

Aim: "fmri resolution at 50Hz"
- strong priors needed!

SBS2: smoothness/ minimum norm
Bayesian inference @ 10 sec.

SBS3: Spike and slab prior
Variational inference @ frame rate,
128 msdelay windows

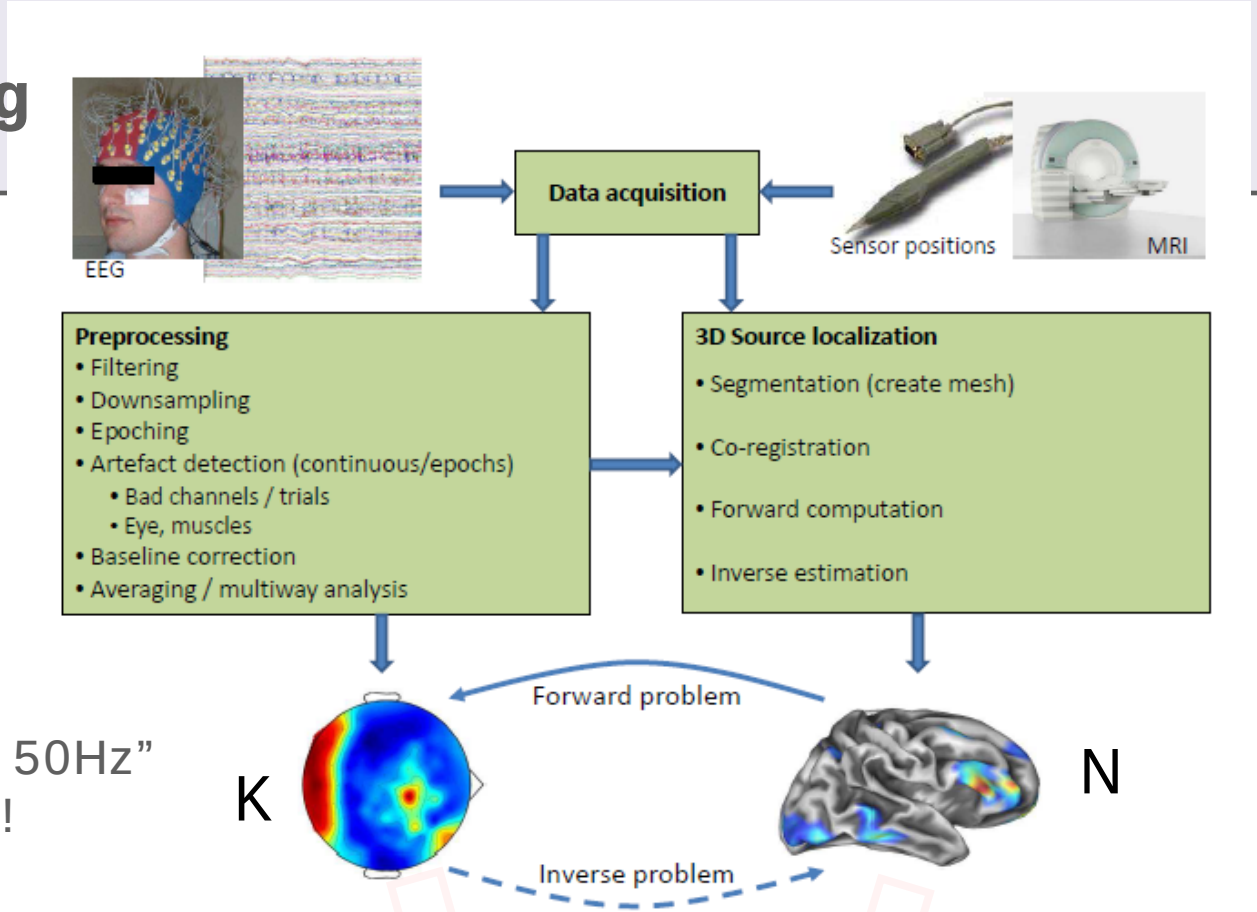

$$Y_{k,t} = \sum_{n=1}^{N} A_{k,n} X_{n,t} + E_{k,t}.$$

ST Hansen, S Hauberg, LK Hansen. Data-driven forward model inference for EEG brain imaging. NeuroImage, 139(1):249-258 (2016)
ST Hansen, LK Hansen. Spatio-temporal reconstruction of brain dynamics from EEG with a Markov prior. NeuroImage, 148:274-283(2017)

SBS2 functions

Real time system

- Bayesian minimum norm 3D reconstruction with a variety of forward models (N=1024).
- Adaptive SNR model (β,α) estimated every 10 sec.
- Update speed ~ 40 fps (Emotiv sample rate 128Hz, blocks of 8 samples)
- Selected frequency band option
- Spatial averaging in ”named” AAL regions

Mobile experiment set-ups, so far…

- Common spatial pattern- BCI
- Stimulus presentation options: video, image, text, audio
- Neuro-feedback

Do we get meaningful functional volumes?

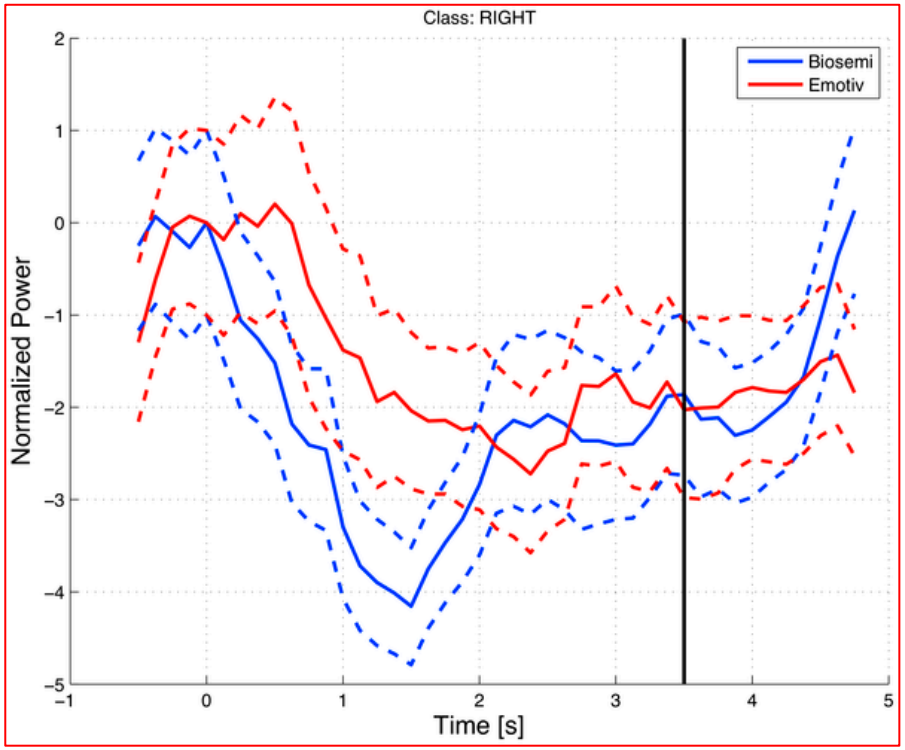

Imagined finger tapping

Left or <u>right</u> cued (at t=0)

Signal collected from an AAL region (n=80)

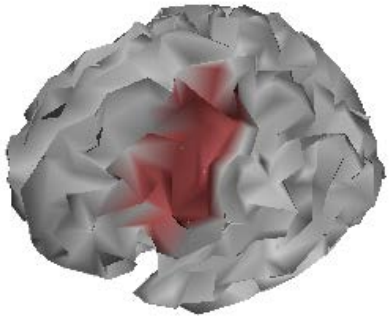

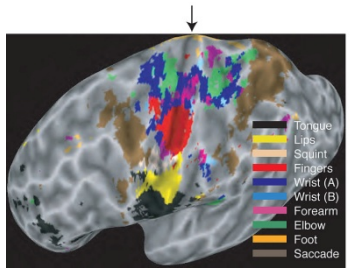

A. Stopczynski, C. Stahlhut, M.K. Petersen, J.E. Larsen, C.F. Jensen, M.G. Ivanova, T.S. Andersen, L.K. Hansen. *Smartphones as pocketable labs: Visions for mobile brain imaging and neurofeedback.* International Journal of Psychophysiology, (2014).

A. Stopczynski, C. Stahlhut, J.E. Larsen, M.K. Petersen, L.K. Hansen. *The Smartphone Brain Scanner: A Portable Real-Time Neuroimaging System.* PloS one 9 (2), e86733, (2014)

Meier, Jeffrey D., Tyson N. Aflalo, Sabine Kastner, and Michael SA Graziano. Complex organization of human primary motor cortex: a high-resolution fMRI study.Journal of neurophysiology 100(4) :800-1812 (2008).

Enabling EEG outside the lab

Mobile real-time EEG Imaging
- -EEG in the classroom
- -Neurofeedback
- -Digital media & emotion
- -Bhutan Epilepsy Project

Simon Kamronn, Andreas Trier Poulsen

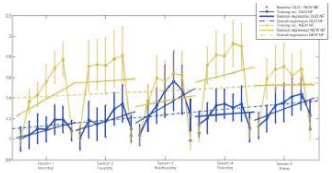

Camilla Falk

SCIENTIFIC REPORTS

OPEN

Validation of a smartphone-based EEG among people with epilepsy: A prospective study

Received: 16 December 2016
Accepted: 27 February 2017
Published: 03 April 2017

Erica D. McKenzie[1], Andrew S. P. Lim[2], Edward C. W. Leung[3], Andrew J. Cole[1], Alice D. Lam[1], Ani Eloyan[4], Damber K. Nirola[5], Lhab Tshering[5], Ronald Thibert[1], Rodrigo Zepeda Garcia[1], Esther Bui[6], Sonam Deki[5], Liesly Lee[2], Sarah J. Clark[1], Joseph M. Cohen[1], Jo Mantia[2], Kate T. Brizzi[1], Tali R. Sorets[1], Sarah Wahlster[7], Mia Borzello[1], Arkadiusz Stopczynski[8], Sydney S. Cash[1] & Farrah J. Mateen[1]

Farrah J. Mateen, Massachusetts General Hospital, Grand Challenges CANADA

SCIENTIFIC REPORTS

OPEN

EEG in the classroom: Synchronised neural recordings during video presentation

Received: 26 April 2016
Accepted: 01 February 2017

Andreas Trier Poulsen[1,*], Simon Kamronn[1,*], Jacek Dmochowski[2,3], Lucas C. Parra[3] & Lars Kai Hansen[1]

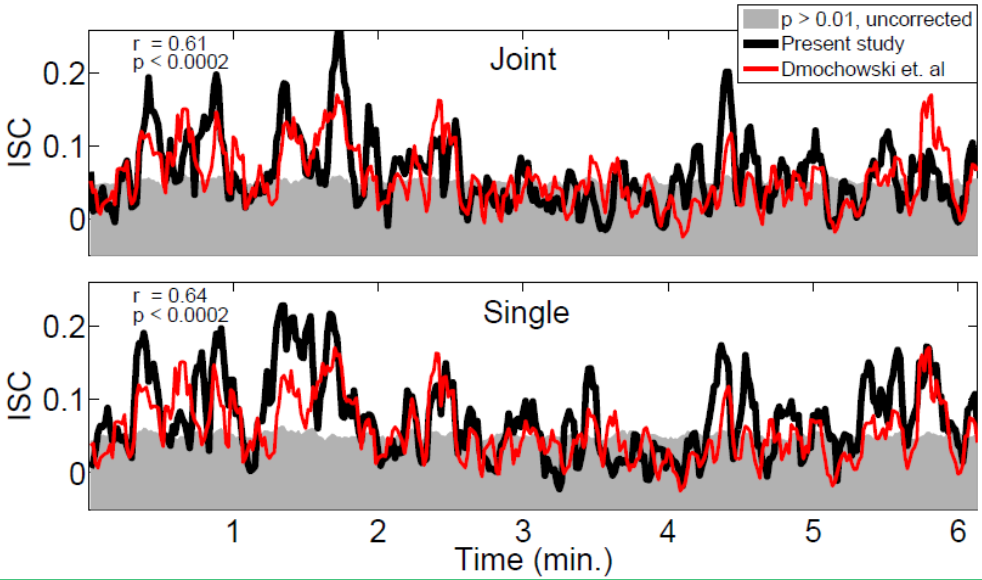

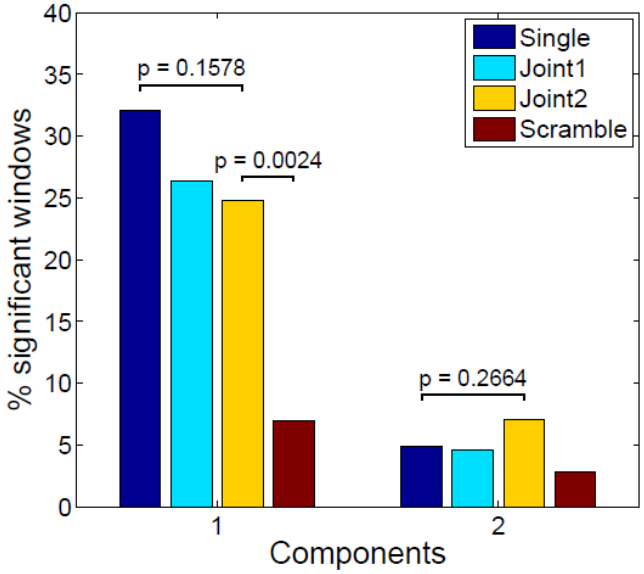

AT Poulsen, S Kamronn, J Dmochowski, LC Parra, LK Hansen. “EEG in the classroom: Synchronised neural recordings during video presentation”. Scientific Reports, 7 (2017).
JP Dmochowski, MA. Bezdek, BP Abelson, JS Johnson, EH Schumacher, LC Parra, ”Audience preferences are predicted by temporal reliability of neural processing”, Nature Communications 5: 4567, July 2014.

Limits to brain state inference:

Time & space

Pushing the limits to imaging with EEG

Lars Kai Hansen
DTU Compute, Technical University of Denmark

Smooth, sparsity promoting priors

Bayesian inference with Variational Garrote

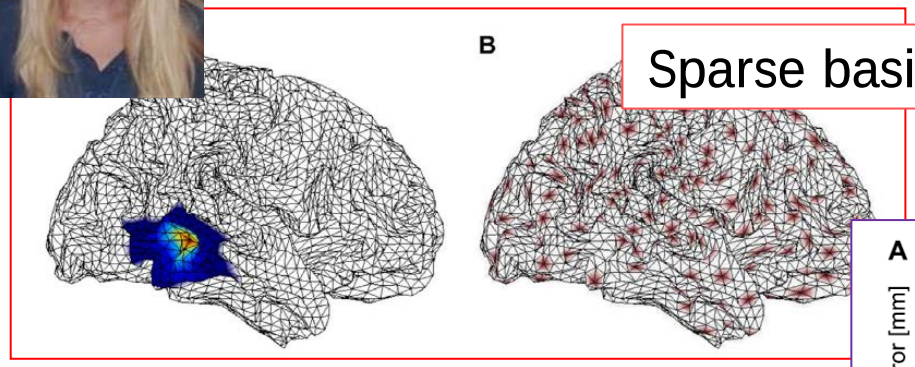

Sparse basis function activity M_{nt} = prob (s_{nt} =1)

$$M_{nt} = \sigma\left(\frac{K\beta}{2}\chi_{nn}X_{nt}^2 + \gamma_1 + \gamma_2(M_{n,t-1} + M_{n,t+1})\right),$$

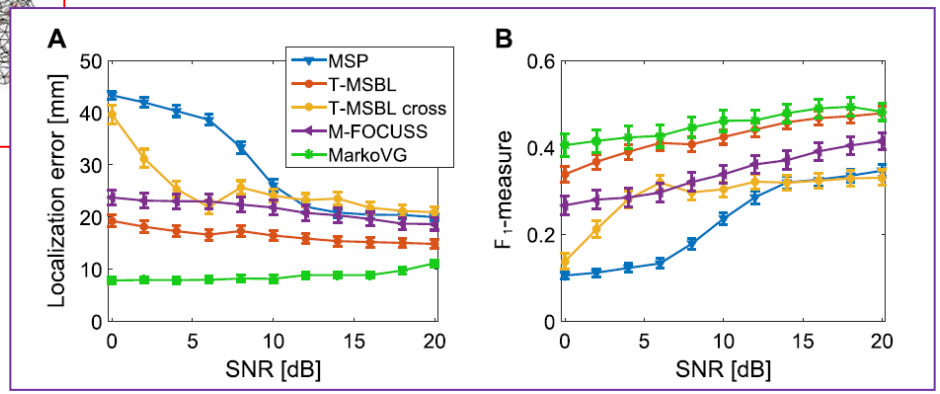

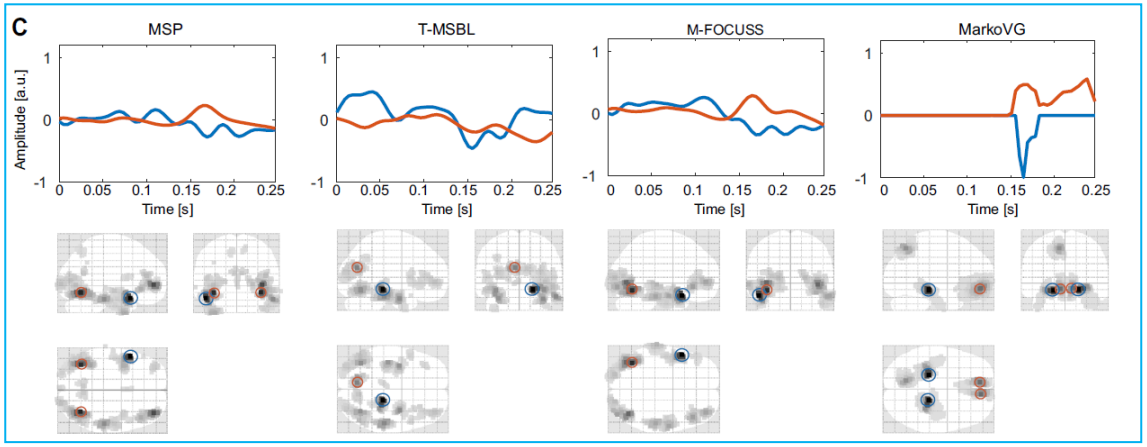

Smartphone brain scanner 3: w/ real-time VG version and artifact reduction

Lars Kai Hansen
DTU Compute, Technical University of

Hansen, S.T. and Hansen, L.K., 2017. *NeuroImage*, *148*, pp.274-283
Spatio-temporal reconstruction of brain dynamics from EEG with a Markov prior.

Reduce limitation to imaging :

Infer the forward model $Y = AX + E$

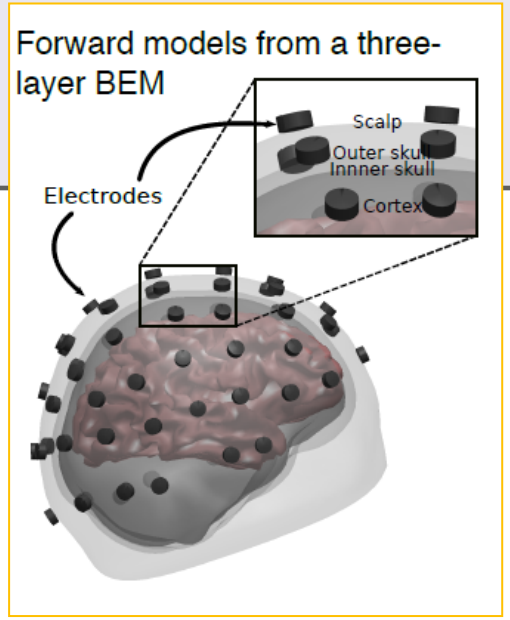

Can we trust the forward model?

- Anatomy is known from MRI, CT?
- Conductivity ratios?

i) Forward model is inaccurate...but useful as ”prior”

- Represent forward model uncertainty as ”naive Bayes” multivariate normal (ARD)
- Estimation embedded with source reconstruction

ii) Data driven approach

- Representing forward model uncertainty as multivariate normal ”probabilistic PCA”
- Estimating embedded with source reconstruction

Reconstruction of the forward model

Uncertainties involved in the estimation of the forward model

- Tissue segmentation
- Tissue conductivities
- Electrode locations

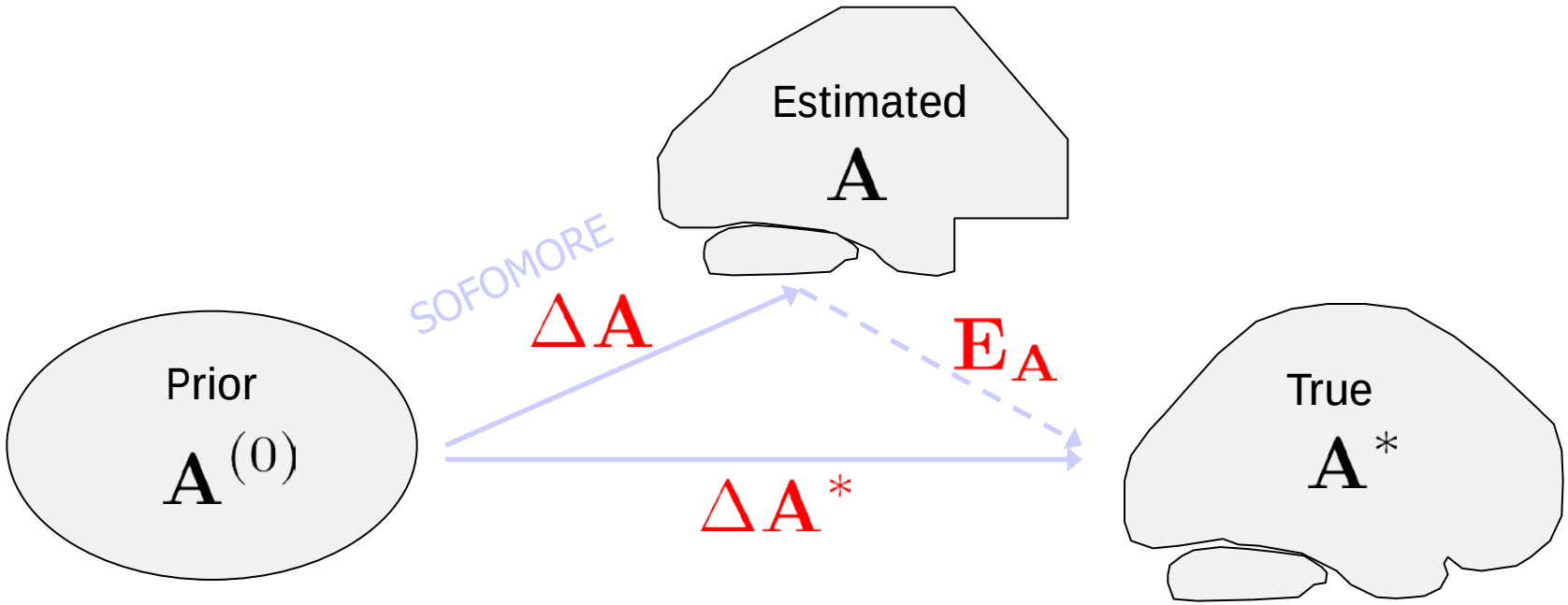

Previous work:

- Gençer & Acar, 2004, Lew et al.,2007; Plis et al., 2007, Acar & Makeig, 2013

C. Stahlhut, M. Mørup, O. Winther, L.K. Hansen. Simultaneous EEG Source and Forward Model Reconstruction (SOFOMORE) using a Hierarchical Bayesian Approach. Journal of Signal Processing Systems, 65(3):431-444 (2011).

The forward model is important!

Magnetoencephalography—theory, instrumentation, and applications to noninvasive studies of the working human brain

Matti Hämäläinen, Riitta Hari, Risto J. Ilmoniemi, Jukka Knuutila, and Olli V. Lounasmaa

Low Temperature Laboratory, Helsinki University of Technology, 02150 Espoo, Finland

Brain Topogr (2013) 26:378–396
DOI 10.1007/s10548-012-0274-6

ORIGINAL PAPER

Effects of Forward Model Errors on EEG Source Localization

Zeynep Akalin Acar · Scott Makeig

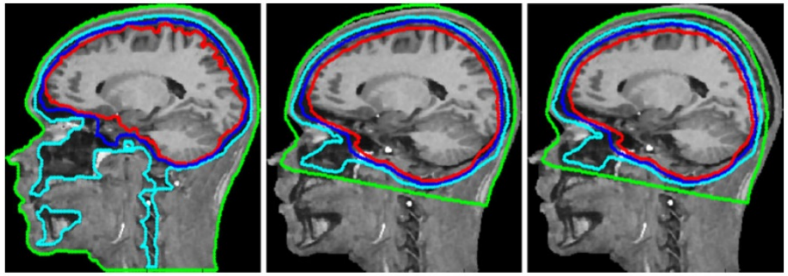

CSF and brain tissue boundaries for **a** four-layer MR-based realistic, **b** four-layer warped MNI, and **c** four-layer MNI head sagittal slice of subject S1

Contents lists available at ScienceDirect

NeuroImage

journal homepage: www.elsevier.com/locate/ynimg

This is an important result because it suggests that creating individual cortical meshes (and all the difficulties that this entails) can be an unnecessary exercise...

Technical Note

Selecting forward models for MEG source-reconstruction using model-evidence

R.N. Henson [a,*], J. Mattout [b], C. Phillips [c], K.J. Friston [d]

IOP PUBLISHING — PHYSICS IN MEDICINE AND BIOLOGY

Phys. Med. Biol. **52** (2007) 5309–5327 — doi:10.1088/0031-9155/52/17/014

Probabilistic forward model for electroencephalography source analysis

Sergey M Plis[1,2], John S George[1], Sung C Jun[1], Doug M Ranken[1], Petr L Volegov[1] and David M Schmidt[1]

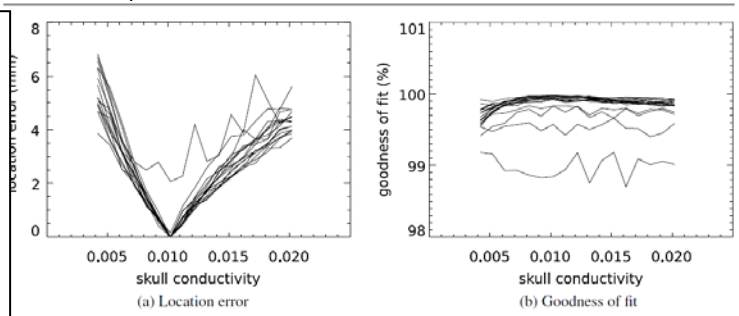

Figure 8. Location error and the corresponding goodness of fit values for 32 single dipole problems simulated with the skull conductivity value set to 0.01021/(Ω m) but analyzed with different fixed values of skull conductivity.

Repairing a wrong forward model with ARD

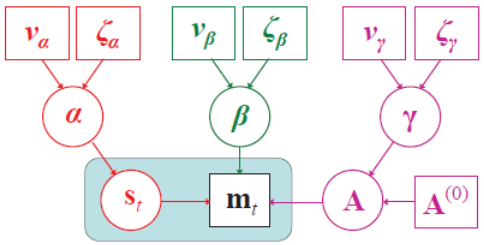

Figure 4.2: **Graphical representation of the SOFOMORE model**. The blue box including the sources $\mathbf{s}_t$ and observations $\mathbf{m}_t$ indicates expansion over time t. At the lowest level in the hierarchical structure we also find the forward model $\mathbf{A}$ with fixed prior mean $\mathbf{A}^{(0)}$. The middle layer includes $\boldsymbol{\alpha}$ precision parameter for the sources with a seperate precision parameter (inverse variance) assigned to each dipole. β is the inverse variance of the noise contribution and $\boldsymbol{\gamma}$ includes a precision parameter to each column in $\mathbf{A}$. At the top level we have the hyperhyperparameters controlling the hyperparameters in the middle layer.

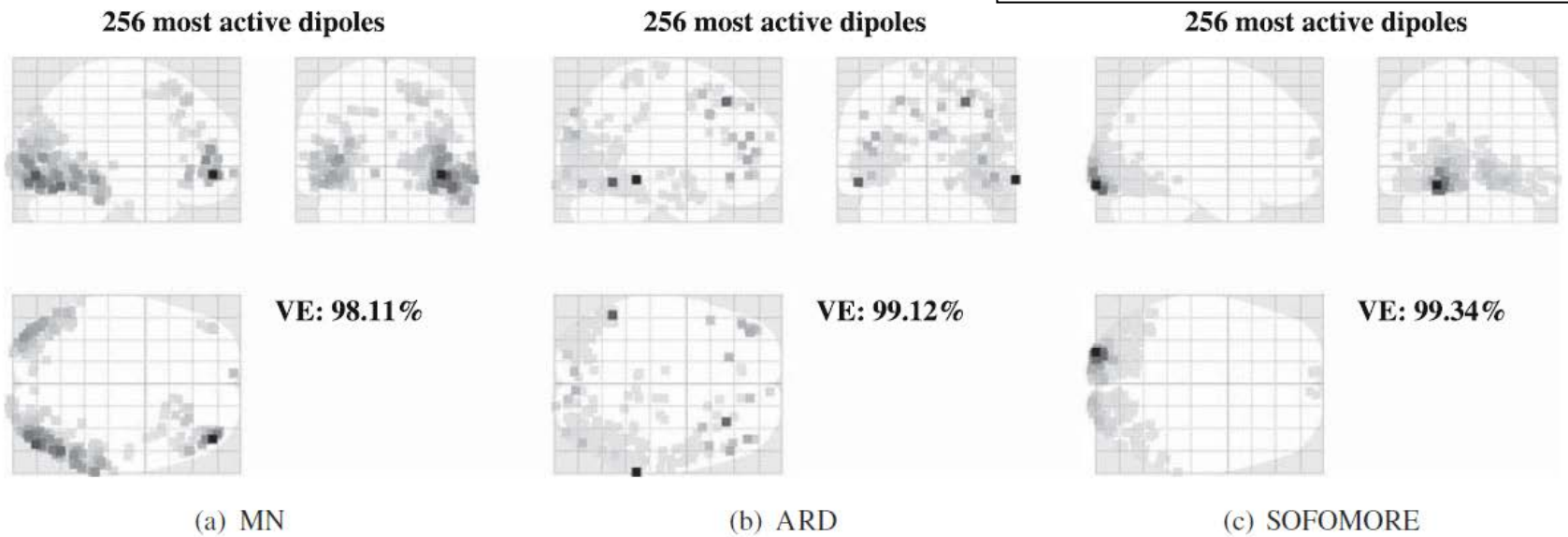

Figure 9 Estimated activity at $t = 170$ ms after stimulus. Tissue conductivities brain:skull:scalp = 0.33:0.0041:0.33 S/m are used. Activity in the left and right occipital region is estimated by MN with the primary activity located in the right occipital region. Moreover, right frontal activity is reconstructed. The ARD leads to quite scattered activity with two dominating dipoles located in the left and right temporal lope. SOFOMORE reconstructs activity both in the left and right visual cortex with dominating activity in the left region.

C. Stahlhut, M. Mørup, O. Winther, L.K. Hansen. Simultaneous EEG Source and Forward Model Reconstruction (SOFOMORE) using a Hierarchical Bayesian Approach. Journal of Signal Processing Systems, 65(3):431-444 (2011).

Representing forward model uncertainty

Can it be estimated even if we do not have anatomy?

A data driven approach

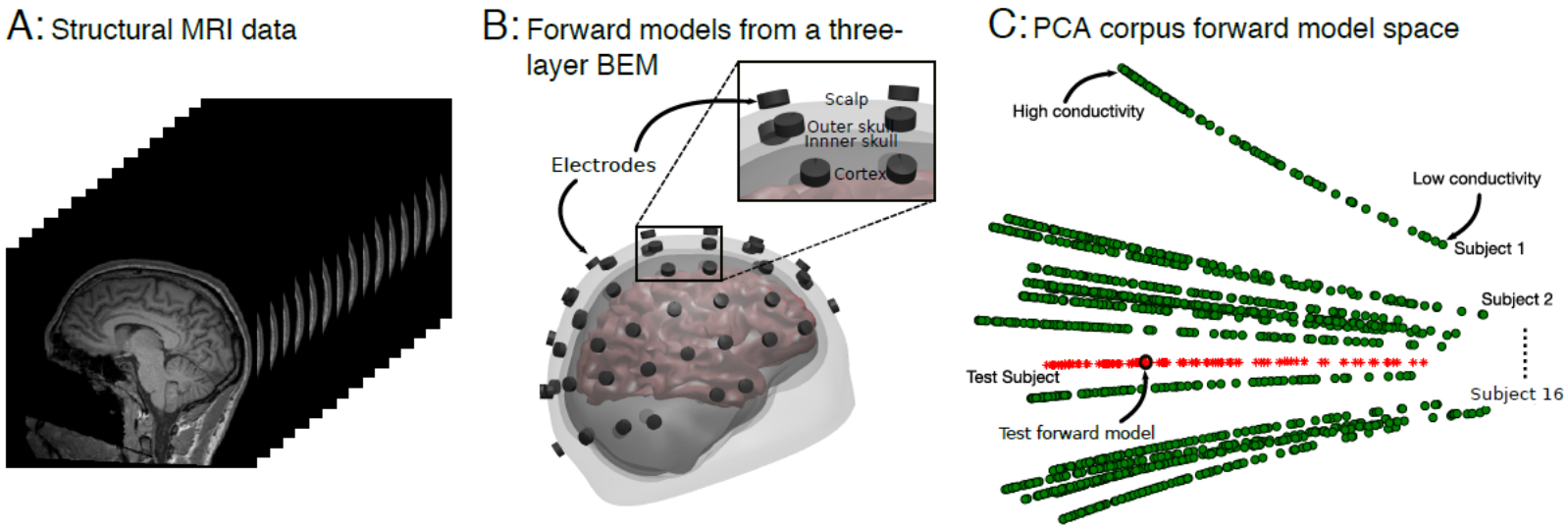

Fig. 1. Illustration of the process of creating forward models and their projection to PCA space. (A) For each of the 16 subjects a T1-weighted image is used to construct a forward model. (B) The forward model is here constructed using a three-layered BEM head model (scalp-skull-brain). For each subject 100 forward models are created, these have varying skull:brain conductivity; from 1 : 250 to 1 : 15. (C) 2D PCA projection of the forward models.

Hansen, S.T., Hauberg, S. and Hansen, L.K., 2016. Data-driven forward model inference for EEG brain imaging. *NeuroImage*, *139*, pp.249-258.

Reducing forward model uncertainty

Augment VG Free energy to incorporate time series and forward model fitness

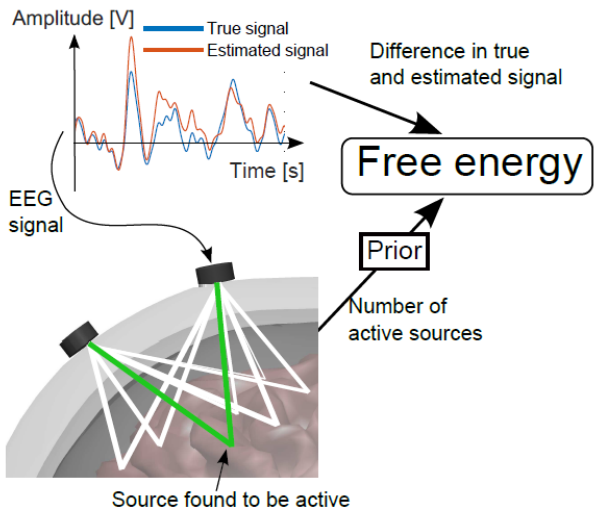

Fig. 2. The Free Energy is a measure of model evidence and expresses the Bayesian combination of data fit (model likelihood), forward model prior distribution based on the forward model corpus, and the source density sparsity promoting prior.

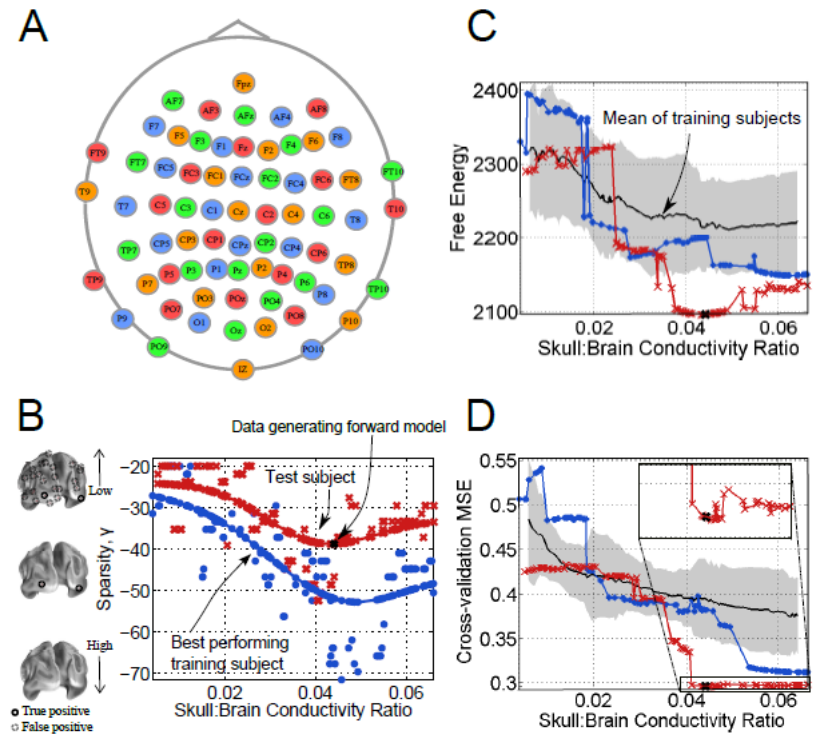

Fig. 3. Recovery of the true forward model among both test and training subjects for simulated data, SNR= 5 dB. (A) The partioning of the 70 10-20 EEG electrodes into four folds. Each color represent one fold. (B) The sparsity levels obtained when running four-fold cross-validation on the test subject (red) and the best performing non-test subject (blue). The found sparsity levels are smoothed across conductivity ratios. (C) The free energy calculated on all electrodes using the smoothed sparsity parameter. (D) The normalized mean squared cross-validation error, also calculated on the smoothed sparsity levels. The mean of the training subjects is shown in black along with the standard deviation in grey. The black 'x' indicates the data generating forward model.

Smooth spatial cross-validation

To estimate regularization (sparsity)

Hansen, S.T., Hauberg, S. and Hansen, L.K., 2016. Data-driven forward model inference for EEG brain imaging. *NeuroImage*, *139*, pp.249-258.

Reducing forward model uncertainty

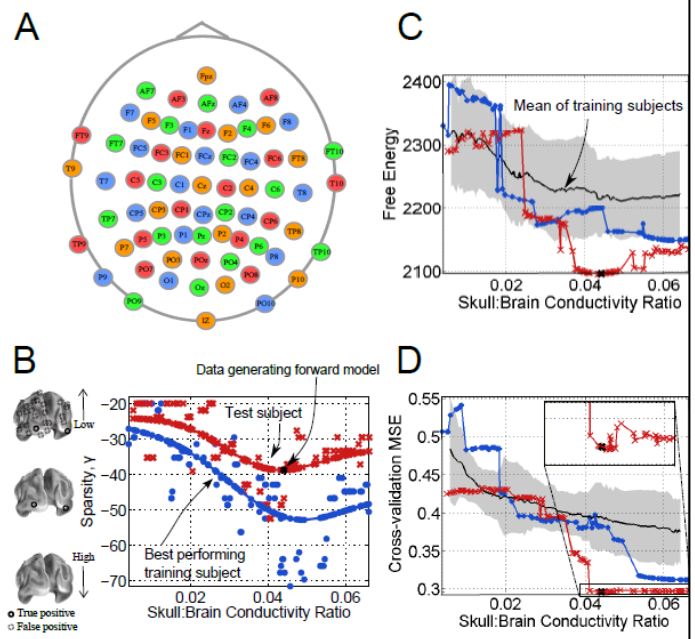

Fig. 3. Recovery of the true forward model among both test and training subjects for simulated data, SNR= 5 dB. (A) The partioning of the 70 10-20 EEG electrodes into four folds. Each color represent one fold. (B) The sparsity levels obtained when running four-fold cross-validation on the test subject (red) and the best performing non-test subject (blue). The found sparsity levels are smoothed across conductivity ratios. (C) The free energy calculated on all electrodes using the smoothed sparsity parameter. (D) The normalized mean squared cross-validation error, also calculated on the smoothed sparsity levels. The mean of the training subjects is shown in black along with the standard deviation in grey. The black 'x' indicates the data generating forward model.

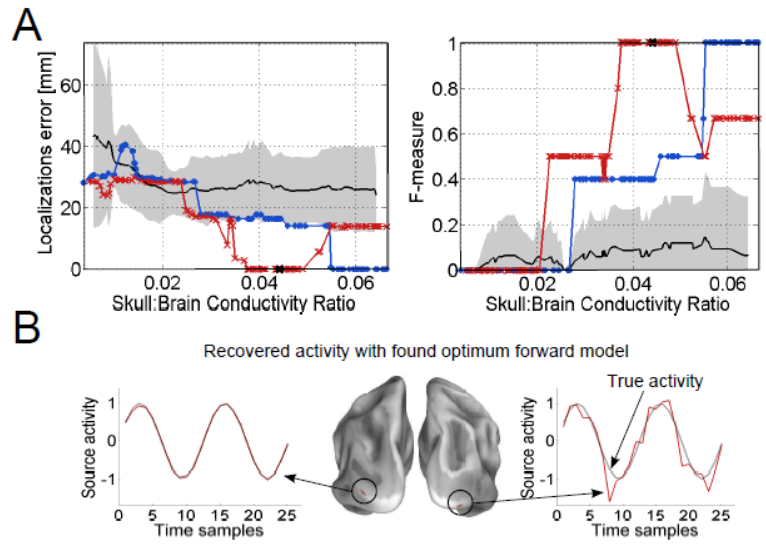

Fig. 4. Recovery of the true forward model among both test and training subjects for simulated data, SNR= 5 dB. (A) The localization error and F-measure for test and best training subject, as well as the mean of all training subjects. Localization error is the sum of the Euclidian distances between planted and strongest reconstructed left and right sources. (B) The source distribution found when using the forward model with lowest free energy. The location of the planted activity is identical to the reconstructed and their sinusoidal development are seen in black.

Smooth spatial cross-validation to estimate regularization (sparsity)
Free energy, cross-validaion, localization error, ”F-measure” all agree

Hansen, S.T., Hauberg, S. and Hansen, L.K., 2016. Data-driven forward model inference for EEG brain imaging. *NeuroImage*, *139*, pp.249-258.

Reducing forward model uncertainty

2D search for forward model in ”PCA space” - leave one-subject-out test **on simulated** data

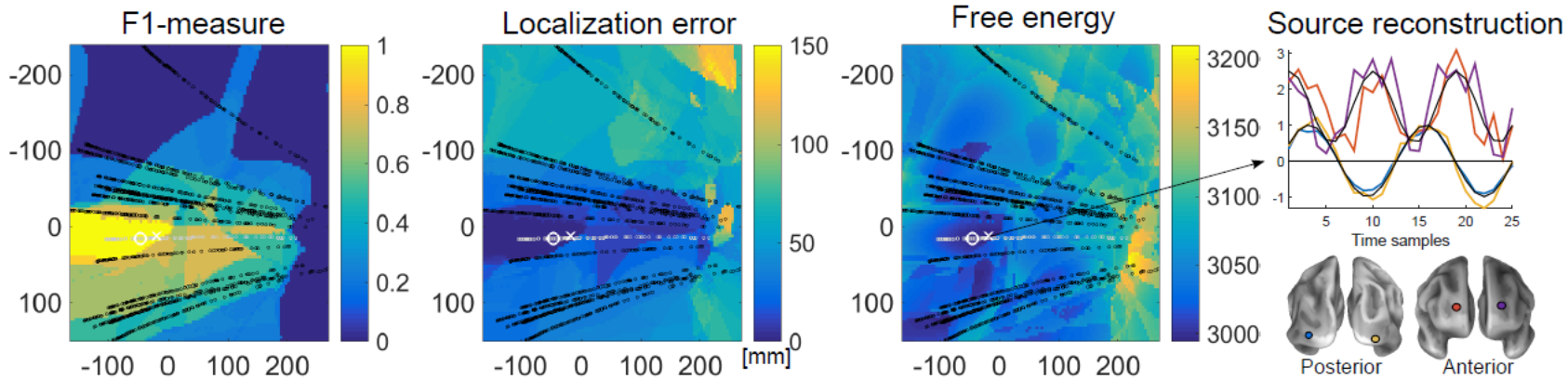

Fig. 5. Search for the optimal forward model in 2D PCA space created by 15 training subjects. A forward model from the sixteenth subject is used to generate the data (same as Fig. 3 and 4). The search space is set to cover the extrema of the forward model PCA projections of the 15 training subjects. The localization error, F-measure, and free energy are overlayed with the forward models of the training subjects in black and test subject in grey. The zoom-in shows the optimum found by the BayesOpt toolbox [45] and the optimum found by 'fminsearch' when using the previous as an initialization. The source reconstruction from the forward model found with these optimizations are also shown.

Hansen, S.T., Hauberg, S. and Hansen, L.K., 2016. Data-driven forward model inference for EEG brain imaging. *NeuroImage*, *139*, pp.249-258.

Reducing forward model uncertainty

2D search for forward model in ”PCA space” - leave one-subject-out test in **real EEG** data

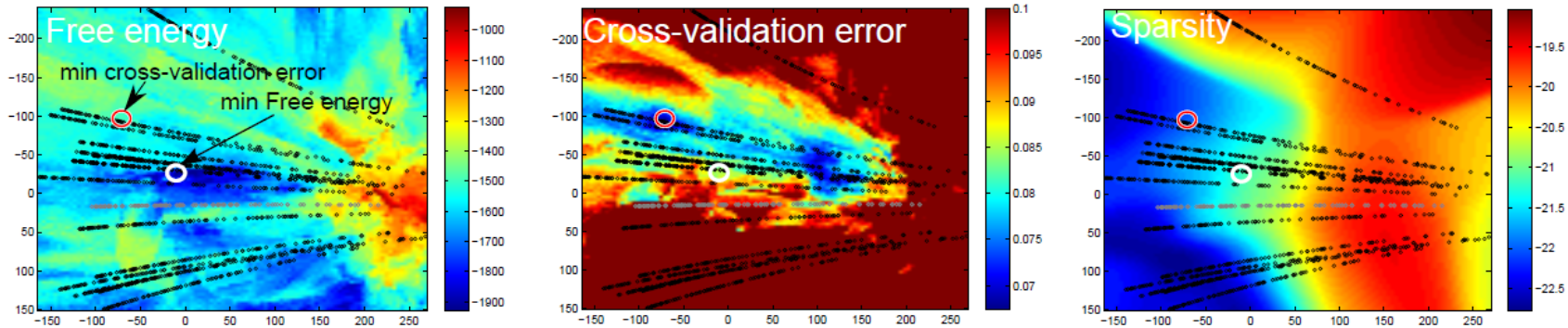

Fig. 7. Search for the optimal forward model in 2D PCA space created by 15 training subjects; real EEG data recorded from the sixteenth subject is applied. The projections of training subjects and the test subject are seen in black and grey, respectively. Due to uncertainty concerning the bandwidth controlling the smoothing of the sparsity, several bandwidths are applied, shown are the averages across these.

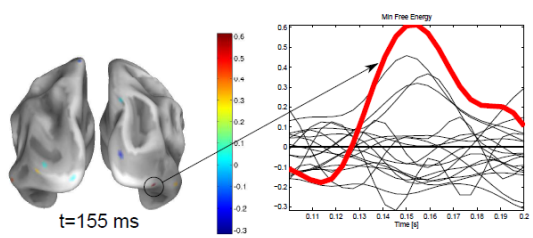

Fig. 6. Source density found at minimum free energy for real EEG data. The location of the strongest source is circled and its activity is depicted in red, the remaining are in black.

Visual processing (face vs non-face)

Test subject activation location well aligned with EEG

Results in state-of-the-art comparison (Henson et al, 2009)

Hansen, S.T., Hauberg, S. and Hansen, L.K., 2016. Data-driven forward model inference for EEG brain imaging. *NeuroImage*, *139*, pp.249-258.

Conclusion

Connect cognitive neuroscience, state monitoring, and daily life

EEG poses many extremely ill-posed problems that limit research and applications

Increasingly sophisticated prior information can help push the limits!

What about the limits to brain state decoding?

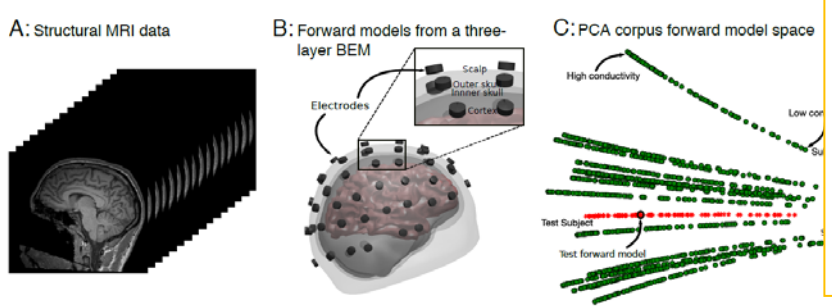

Fig. 1. Illustration of the process of creating forward models and their projection to PCA space. (A) For each of the 16 subjects a T1-weighted image is used to construct a forward model. (B) The forward model is here constructed using a three-layered BEM head model (scalp-skull-brain). For each subject 100 forward models are created, these have varying skull:brain conductivity; from 1 : 250 to 1 : 15. (C) 2D PCA projection of the forward models.

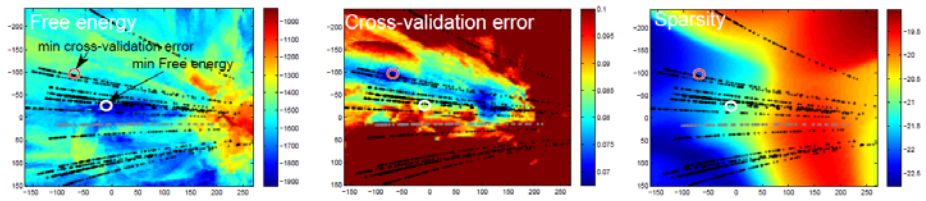

Fig. 7. Search for the optimal forward model in 2D PCA space created by 15 training subjects; real EEG data recorded from the sixteenth subject is applied. The projections of training subjects and the test subject are seen in black and grey, respectively. Due to uncertainty concerning the bandwidth controlling the smoothing of the sparsity, several bandwidths are applied, shown are the averages across these.

Are there limits to decoding?

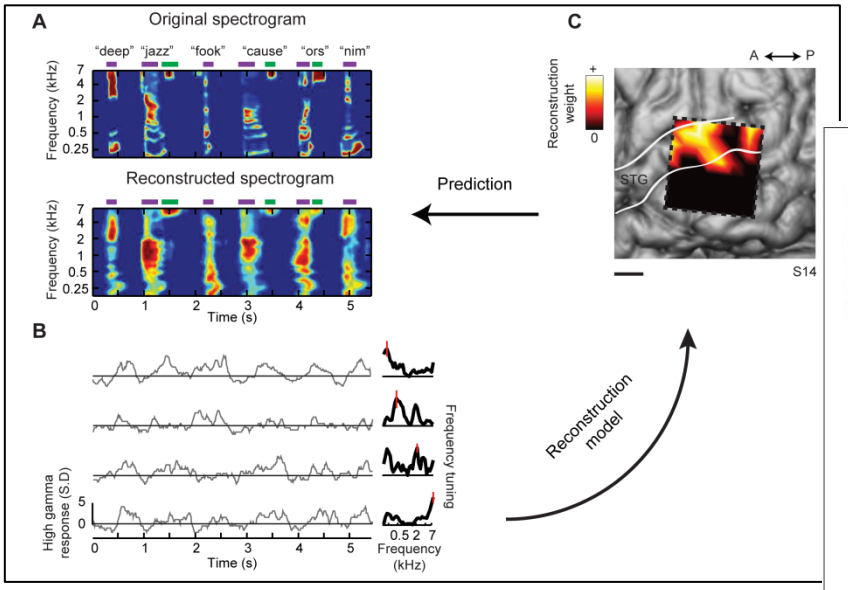

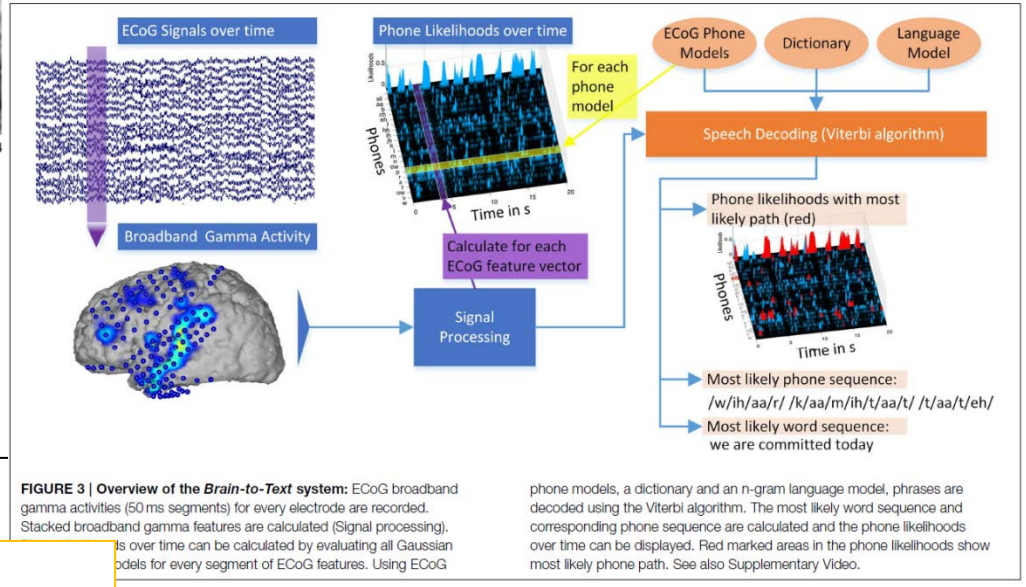

FIGURE 3 | Overview of the *Brain-to-Text* system: ECoG broadband gamma activities (50 ms segments) for every electrode are recorded. Stacked broadband gamma features are calculated (Signal processing). ...ds over time can be calculated by evaluating all Gaussian ...odels for every segment of ECoG features. Using ECoG phone models, a dictionary and an n-gram language model, phrases are decoded using the Viterbi algorithm. The most likely word sequence and corresponding phone sequence are calculated and the phone likelihoods over time can be displayed. Red marked areas in the phone likelihoods show most likely phone path. See also Supplementary Video.

ARTICLE

Received 15 Oct 2015 | Accepted 21 Feb 2017 | Published 22 May 2017 DOI: 10.1038/ncomms15037 OPEN

Generic decoding of seen and imagined objects using hierarchical visual features

Tomoyasu Horikawa[1] & Yukiyasu Kamitani[1,2]

Kamitani, fMRI "Our results demonstrate a homology between human and machine vision and its utility for brain-based information retrieval."

Pasley, B.N., David, S.V., Mesgarani, N., Flinker, A., Shamma, S.A., Crone, N.E., Knight, R.T. and Chang, E.F., 2012. Reconstructing speech from human auditory cortex. *PLoS biology*, *10*(1), p.e1001251

Herff, C., Heger, D., de Pesters, A., Telaar, D., Brunner, P., Schalk, G. and Schultz, T., 2015. Brain-to-text: decoding spoken phrases from phone representations in the brain. *Frontiers in neuroscience*, *9*.